

Emission spectrum and quenching kinetics of Xe_2F^*

W. Walter,^{a)} R. Sauerbrey,^{a)} F. K. Tittel, and W. L. Wilson, Jr.

Electrical Engineering Department and Rice Quantum Institute, Rice University, P. O. Box 1892, Houston, Texas 77251

(Received 5 April 1982; accepted for publication 22 June 1982)

Experiments demonstrating the existence of the triatomic rare-gas excimer Xe_2F^* are reported. Three-body quenching of $\text{XeF}^*(B,C)$ yields Xe_2F^* , which radiates around 610 nm with a bandwidth full width at half-maximum (FWHM) of 120 nm. The two-body quenching constants of Xe_2F^* by NF_3 , Xe, and Ar as well as the radiative lifetime of 152 ns are determined.

PACS numbers: 42.65.Cq, 42.55.Hq

In recent years the kinetic processes leading to the formation and quenching of the rare-gas halide molecule XeF^* have been investigated by several groups using different excitation techniques.¹⁻⁴ The kinetic reactions of XeF^* are complicated by the fact that the lowest excited state $\text{XeF}(C,^2\Pi)$ lies below the $\text{XeF}(B,^2\Sigma^+)$ state by about 600 to 700 cm^{-1} .^{3,4} This was not taken into account in the early works.^{1,2} Three-body quenching rate constants for XeF^* have been measured by several authors^{1,2,4} but they differ by several orders of magnitude. The most likely product for three-body quenching of $\text{XeF}^*(B,C)$, involving at least one Xe atom, would be Xe_2F^* . Although many triatomic rare-gas halides have been observed,⁵ previous attempts to observe Xe_2F^* have been unsuccessful.^{1,3,4}

In this letter considerable three-body quenching of XeF^* in electron beam excited high pressure Xe- NF_3 and in Ar-Xe- NF_3 mixtures is demonstrated. Furthermore, optical emission from a red continuum assigned to Xe_2F^* has been recorded, and the most important two-body quenching rate constants, as well as the radiative lifetime of Xe_2F^* , have been measured for the first time.

Details of the experimental apparatus have been described elsewhere.⁵ Gas mixtures consisting of high purity argon (99.9995%) or neon (99.9996%), xenon (99.995%) and NF_3 (99.5%) were transversely pumped by a pulsed electron beam. The typical maximum electron current density on the optical axis of the gas cell was 200 A/cm^2 as measured by a Faraday cup probe. The maximum electron energy was 1 MeV and the pulse width was 10 ns. An area of 10×2 cm was irradiated by the electron beam. The time integrated fluorescence spectra were recorded by an optical multichannel analyzer (OMA1) using a 0.25-nm Jarrel-Ash spectrometer with a 2-nm resolution. The time dependence of the fluorescence of the $\text{XeF}(B \rightarrow X)$ and $\text{XeF}(C \rightarrow A)$ transitions at 350 and 475 nm, respectively, as well as the red continuum at 610 nm, was measured using either a fast vacuum photodiode (ITT F4000S) or a photomultiplier (RCA C3100A). Spectral selection was obtained with appropriate interference and color glass filters. The fluorescence pulses were recorded by a transient digitizer (Tektronix 7912). The rise time of the photodiode detecting system was < 2 ns and that of the photomultiplier as less than 5 ns. The data from the OMA and the transient digitizer were stored and processed by a PDP11/23 minicomputer.

^{a)} Permanent address: Physikalisches Institut der Universität Würzburg, 8700 Würzburg, Federal Republic of Germany.

In order to investigate reactions of XeF^* with other components of the gas mixture, vibrational relaxation in the electronic states and mixing between the C and B states by collisions with atoms or electrons must be taken into account.^{3,4} A detailed analysis of these processes will be discussed later. In this letter the discussion, as far as XeF^* is concerned, is restricted mainly to qualitative aspects.

Figure 1 shows the spectra of both an electron beam excited Ar-Xe- NF_3 from 250 to 720 nm and a Xe- NF_3 mixture from 470 to 720 nm. The relative intensities have been corrected for the OMA1 spectral sensitivity. The $D \rightarrow X$ and $B \rightarrow X$ transitions of XeF^* appear at 265 and 352 nm, respectively. Vibrational structure in these transitions is not resolved. In the spectral region from 420 to 720 nm a broad continuum is observed. In the case of the Ar-Xe- NF_3 mixture it consists of two components, a short wavelength part peaks at 475 nm, and a second broad continuum appears around 600 nm. The intensity of this continuum increases sharply with increasing xenon pressure.

In the high pressure Xe- NF_3 mixture the 475-nm emission is very low. Only the red continuum appears with its peak located at (610 ± 10) nm and a spectral width of (130 ± 10) nm. Similar spectra are also obtained in Ar-Xe- NF_3 mixtures with 6 atm Ar, 10 Torr NF_3 , and more than 300 Torr Xe. When the xenon pressure is reduced below 30 Torr essentially only the blue-green continuum can be observed. The blue-green fluorescence has been assigned to the bound free $C \rightarrow A$ transition of XeF^* .^{4,5}

From measurements at low xenon pressures (< 30 Torr) when the intensity of the red emission is negligibly small the

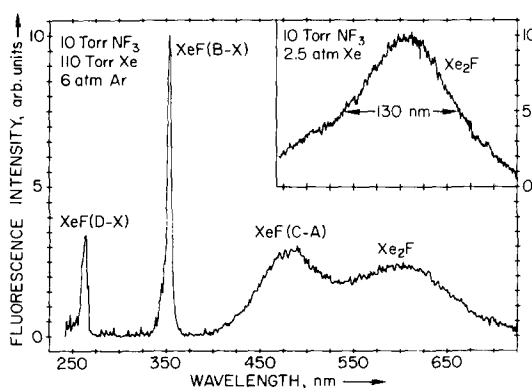


FIG. 1. Spectrum of an electron beam excited Ar-Xe- NF_3 mixture and a Xe- NF_3 mixture. The intensities are corrected for the spectral sensitivity of the OMA1 detection system.

spectral shape of the $\text{XeF}(C \rightarrow A)$ emission can be determined. Because of the high argon pressure (6 atm) the vibrational relaxation of the C state occurs very rapidly and thus the spectral width of this transition becomes independent of the xenon pressure. Therefore the spectra between 420 and 720 nm can be subtracted appropriately yielding the spectral shape of the red emission. Preliminary results are (612 ± 5) nm for the peak wavelength and (120 ± 5) nm for the spectral bandwidth full width at half-maximum (FWHM). This is in good agreement with values determined from $\text{Xe}-\text{NF}_3$ mixtures at high xenon pressures (Fig. 1). Spectra similar to those obtained using $\text{Ar}-\text{Xe}-\text{NF}_3$ mixtures were also observed when using $\text{Ne}-\text{Xe}-\text{NF}_3$ mixtures. However, quantitative measurements on these were complicated by very intense emissions from many lines between 500 and 700 nm due to radiative transitions in neon.

The temporal dependence of the fluorescence behavior of $\text{XeF}(B \rightarrow X)$, $\text{XeF}(C \rightarrow A)$ and the red emission at 610 nm are shown in Fig. 2. By using appropriate interference and color glass filters, care was taken not to measure the time dependences in the overlapping wavelength region of the two continua. At low xenon pressures (less than 20 Torr in 6 atm argon), competing signals from argon transitions were superimposed onto the red fluorescence signal, but their rapid decay time allowed a subtraction of the argon fluorescence (Fig. 2).

A steep onset of the $B \rightarrow X$ transition is shown in Fig. 2, whereas the $C \rightarrow A$ fluorescence appears somewhat delayed. This behavior is characteristic for electron beam excited $\text{Ar}-\text{Xe}-\text{NF}_3$ mixtures and seems to indicate that the B level of XeF^* is produced first. Subsequently the population of the C level increases due to collisional mixing of both states. This phenomenon was also observed by Brashears and Setser⁴ using photolytic excitation. The decay of both states was found to be equal within the experimental errors at high argon pressures indicating the existence of thermal equilibrium between the two states during their decay.

In $\text{Xe}-\text{NF}_3$ mixtures the $B \rightarrow X$ and the $C \rightarrow A$ transitions showed exactly the same time dependence if the xenon pressure was greater than 100 Torr. Thus, one has to conclude that collisional mixing between the two states with xenon is much faster than with argon.

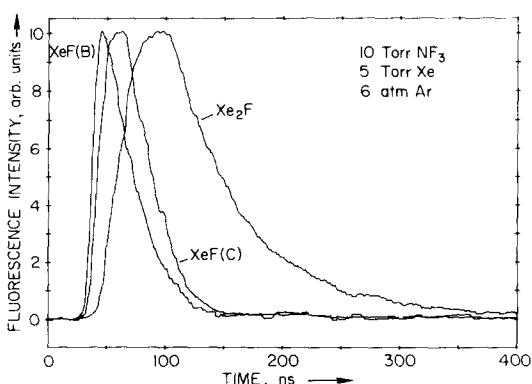


FIG. 2. Time-resolved fluorescence from $\text{XeF}(B \rightarrow X)$, $\text{XeF}(C \rightarrow A)$, and Xe_2F^* . The fluorescence pulses are normalized to the same relative intensity. The red argon fluorescence was subtracted from the Xe_2F^* spontaneous emission signal.

The intensity of the red continuum increases until the $\text{XeF}(B \rightarrow X)$ and $\text{XeF}(C \rightarrow A)$ pulses have nearly decayed. This characteristic is consistent with the production of this red emitter from these states. The decay of the red emission is considerably slower than for the two XeF^* transitions, indicating a comparatively long radiative lifetime.

In order to study the quenching mechanisms of XeF^* , collisional mixing of the B and C states has to be taken into account. When the analysis is restricted to $\text{Xe}-\text{NF}_3$ mixtures, two-body quenching of both states by NF_3 and Xe and possibly three-body quenching by Xe have to be considered. The rate equations for the two states can be written as follows:

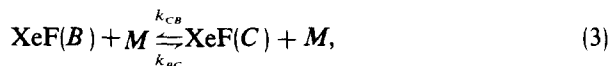
$$\frac{d[B]}{dt} = P_B + k_{CB}[M][C] - k_{BC}[M][B] - \frac{1}{\tau_1}[B], \quad (1)$$

$$\frac{d[C]}{dt} = P_C + k_{BC}[M][B] - k_{CB}[M][C] - \frac{1}{\tau_2}[C], \quad (2)$$

$$\frac{1}{\tau_1} = \frac{1}{\tau_B} + k_B^{\text{NF}_3}[\text{NF}_3] + k_B^{\text{Xe}}[\text{Xe}] + k_B^{2\text{Xe}}[\text{Xe}]^2,$$

$$\frac{1}{\tau_2} = \frac{1}{\tau_C} + k_C^{\text{NF}_3}[\text{NF}_3] + k_C^{\text{Xe}}[\text{Xe}] + k_C^{2\text{Xe}}[\text{Xe}]^2.$$

The quantities in brackets denote the concentrations of the corresponding species. P_B and P_C are the production rates of the B and C states, respectively. τ_B , τ_C are the radiative lifetimes and k_B^Q , k_C^Q the quenching constants involving the species Q for the two states, respectively. The mixing constants k_{BC} and k_{CB} characterize the reaction



where M is any collision partner inducing mixing, primarily xenon in this case or possibly an electron.

Although (1) and (2) can be solved exactly when the production rates are known, in this work only a simple approximate solution is developed in order to demonstrate that there is considerable three-body quenching of XeF^* by Xe . As mentioned earlier in the case of $\text{Xe}-\text{NF}_3$ mixtures, the fluorescence pulse of the $B \rightarrow X$ and the $C \rightarrow A$ transitions had identical pulse shapes. This indicates tight coupling of the two states. Thus, assuming that collisional mixing is much faster than the other quenching and decay processes, the concentrations of the two states should have their equilibrium ratio: $[B]/[C] = k_{CB}/k_{BC}$. Introducing this approximation into (1) and (2) and adding both equations yields

$$\frac{d[B]}{dt} = \left(1 + \frac{k_{BC}}{k_{CB}}\right)^{-1} \left[P_B - \left(\frac{1}{\tau_1} + \frac{k_{BC}}{k_{CB}} \frac{1}{\tau_2} \right) [B] \right]. \quad (4)$$

Here, direct production of the C state has been neglected.

Assuming that the production rate of $\text{XeF}(B)$ in a xenon atmosphere is proportional to the xenon pressure, and noting that $d[B]/dt = 0$ at a temporal maximum, one obtains

$$[Xe]/U_{\text{max}}^B = a + b[Xe] + c[Xe]^2, \quad (5)$$

where u_{max}^B represents the maximum intensity of the $B \rightarrow X$

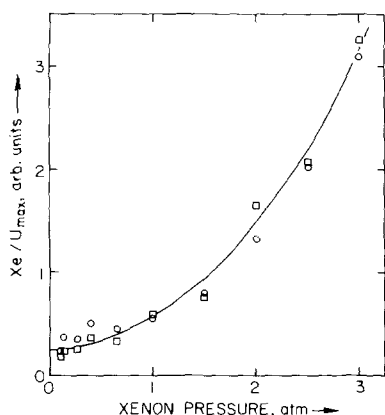


FIG. 3. Dependence of Xe/U_{max} on the xenon pressure. Circles (O) denote the $C \rightarrow A$ transition, and squares (\square) depict the $B \rightarrow X$ transition. The solid curve is a quadratic polynomial [Eqs. (5) and (6)] with $a = 0.25$, $b = 0$ atm^{-1} , and $c = 0.31$ atm^{-2} .

fluorescence, and a, b, c are constants obtained from the expansion of τ_1^{-1} and τ_2^{-1} . a contains the radiative lifetimes and the NF_3 quenching constants, b the two-body xenon quenching constants, and c the three-body xenon quenching constants. Because $[B]/[C] = \text{constant}$ for all times especially at the fluorescence maximum, it follows for the temporal maximum of the $C \rightarrow A$ fluorescence U_{max}^C :

$$[Xe]/U_{max}^C = a' + b'[Xe] + c'[Xe]^2. \quad (6)$$

The constants a, b, c should be related to a', b', c' by the same scale factor. Therefore, the appropriately scaled values of $[Xe]/U_{max}^B$ and $[Xe]/U_{max}^C$ should yield the same xenon pressure dependence. This ratio is shown for the B and C states in Fig. 3. It has indeed the same pressure dependence for both levels. The experimental points can obviously not be fitted by a straight line. However, a second-order polynomial provides an excellent fit to the experimental results. Therefore, it may be concluded that XeF^* is quenched by Xe in a three-body collision, indicating a complex formation of XeF^* with xenon.

It is difficult to obtain an exact value for the three-body rate constant from this fit because of a lack of knowledge of k_{BC}/k_{CB} . It is not clear if the mixing between the B and the C states is mainly caused by secondary electrons or by collision with other atoms or molecules. The question of vibrational relaxation in these states causes further complications. Assuming that electrons are responsible for the mixing and that the population of both electronic states is mainly in the lowest vibrational level, the three-body quenching constant of the B state can be estimated to be $2.10^{-31} \text{ cm}^6 \text{ s}^{-1}$.

Considering the experimental and theoretical uncertainties, this is in reasonable agreement with the value of $2.6 \times 10^{-31} \text{ cm}^6 \text{ s}^{-1}$ measured by Trainor *et al.*² and an upper limit for this constant of $3 \times 10^{-31} \text{ cm}^6 \text{ s}^{-1}$ reported by Brashears and Setser⁴ but differs from the value of $2.4 \times 10^{-29} \text{ cm}^6 \text{ s}^{-1}$ given in Ref. 1.

In similar electron beam pumped systems, broadband emissions with properties analogous to the red emission have been assigned to the triatomic rare-gas halides.⁵ So it may be concluded that the observed red fluorescence is due to Xe_2F^* . Mixed triatomic excimers like ArXeF^* can be ex-

cluded because the red continuum was also observed in Xe-NF_3 mixtures. The Xe_2F^* emission wavelength was calculated by Huestis³ to lie between 615 and 808 nm. The lower bound of this calculation is in agreement with the measured value of $(612 \pm 5) \text{ nm}$. In accordance with these calculations, it can be assumed that the lowest excited state of Xe_2F^* decays to a steeply repulsive ground-state potential curve causing emission of radiation in a very broad band.

The relationship between the temporal behavior of the Xe_2F^* fluorescence and that of the XeF^* fluorescence and the observed considerable three-body quenching of XeF^* , indicates that XeF^* is the main precursor of Xe_2F^* . Precursors with a long lifetime like Xe_2^* would yield delayed fluorescence components and a complicated decay of the fluorescence signal. However, after the $\text{XeF}(B \rightarrow X)$ and $\text{XeF}(C \rightarrow A)$ emissions have decayed to zero, pure exponential decays of Xe_2F^* have always been observed. Thus the effective decay time τ_{eff} of the lowest excited state of Xe_2F^* may be written in the form

$$1/\tau_{\text{eff}} = 1/\tau_{\text{Xe}_2\text{F}^*} + k^{\text{NF}_3}[\text{NF}_3] + k^{\text{Xe}}[\text{Xe}] + k^{\text{Ar}}[\text{Ar}], \quad (7)$$

where $\tau_{\text{Xe}_2\text{F}^*}$ is the radiative lifetime of Xe_2F^* and the constants k^Q are the quenching rate constants of Xe_2F^* by the corresponding species Q . Hence, the radiative lifetime and the quenching constants can be determined by measuring the effective lifetime of the Xe_2F^* fluorescence as a function of the partial pressures of the difference species in the gas mixture. From appropriate Stern-Volmer plots, the following results have been determined: $k^{\text{NF}_3} = (7.8 \pm 1.2) \times 10^{-13} \text{ cm}^3 \text{ s}^{-1}$, $k^{\text{Xe}} = (1.0 \pm 0.2) \times 10^{-13} \text{ cm}^3 \text{ s}^{-1}$, $k^{\text{Ar}} = (2.9 \pm 0.9) \times 10^{-14} \text{ cm}^3 \text{ s}^{-1}$, and $\tau_{\text{Xe}_2\text{F}^*} = (152 \pm 10) \text{ ns}$.

In conclusion, it has been demonstrated that the intense broadband red emission in electron beam excited xenon containing rare-gas- NF_3 mixtures is due to Xe_2F^* . The emission spectrum as well as the radiative lifetime and several quenching constants of the lowest excited state of Xe_2F^* were determined. The detailed production mechanism of Xe_2F^* is not as yet understood; however, an analysis that considers the complicated behavior of its most likely precursor XeF^* , is presently in progress.

This research was jointly supported by the Office of Naval Research, the National Science Foundation and the Robert A. Welch Foundation. R. Sauerbrey would like to acknowledge support by the Deutsche Forschungsgemeinschaft.

¹J. G. Eden and R. W. Wayant, *J. Chem. Phys.* **68**, 2850 (1978); J. G. Eden and R. W. Wayant, *Opt. Lett.* **2**, 13 (1978).

²M. Rokni, J. H. Jacob, J. C. Hsia, and D. W. Trainor, *Appl. Phys. Lett.* **35**, 729 (1979); D. W. Trainor, J. H. Jacob, and M. Rokni, *J. Chem. Phys.* **72**, 3646 (1980); M. Rokni, J. H. Jacob, J. A. Mangano, and R. Brochu, *Appl. Phys. Lett.* **32**, 223 (1978); M. Rokni, J. H. Jacob, J. A. Mangano, and R. Brochu, *Appl. Phys. Lett.* **30**, 458 (1977).

³G. Black, R. L. Sharpless, D. C. Lorents, D. L. Huestis, R. A. Gutcheck, T. D. Bonifield, D. A. Helms, and G. K. Walters, *J. Chem. Phys.* **75**, 4840 (1981).

⁴H. C. Brashears, Jr. and D. W. Setser, *J. Chem. Phys.* **76**, 4932 (1982); H. C. Brashears, Jr. and D. W. Setser, *Appl. Phys. Lett.* **33**, 821 (1978).

⁵F. K. Tittel, G. Marowsky, W. L. Wilson, Jr., and M. C. Smayling, *IEEE J. Quantum Electron.* **QE-12**, 2268 (1981).